

NASA Technical Memorandum 104162

11-64
51754
P-19

**A Fourier Collocation Time Domain Method
for Numerically Solving Maxwell's Equations**

(NASA-TM-104162) A FOURIER COLLOCATION TIME
DOMAIN METHOD FOR NUMERICALLY SOLVING
MAXWELL'S EQUATIONS (NASA) 19 p CSCL 12A

N92-11742

Unclas
G3/64 0051754

John V. Shebalin

October 1991



National Aeronautics and
Space Administration

Langley Research Center
Hampton, Virginia 23665-5225

Abstract

A new method for solving Maxwell's equations in the time domain for arbitrary values of permittivity, conductivity, and permeability is presented. Spatial derivatives are found by a Fourier transform method and time integration is performed using a second-order, semi-implicit procedure. Electric and magnetic fields are collocated on the same grid points, rather than on interleaved points, as in the finite difference time domain (FDTD) method. Numerical results for the propagation of a 2-D TEM mode out of a parallel plate wave guide and into a dielectric and conducting medium is presented.

Introduction

Solving Maxwell's equations by finite difference procedures in the time domain has been steadily gaining popularity since the pioneering work of Yee [1] and Taflove [2]; a good example (with more references) of this finite difference time domain (FDTD) method is given in the recent work of Britt [3]. Here, we present the beginnings of a new method, a Fourier collocation time domain (FCTD) approach. We will concentrate here on two-dimensional (2-D) simulations, as these provide a good compromise between reality and resolution; 1-D and 3-D simulations are straightforward extensions of the results presented here.

First, we will define our coordinate system and model problem, and second, set up the 2-D system of Maxwell's equations which we wish to solve. Third, we will explicitly discuss the FCTD method of solution. Fourth, we will present numerical results, and lastly, give a summary and conclusion.

Problem Definition

The physical problem we are attempting to solve by numerical simulation consists of a microwave horn emitting a single frequency, continuous wave signal through a dielectric slab and into a plasma. The motivation for this problem is the planned use of a microwave reflectometer to determine critical electron number densities in the stagnation region of hypersonic reentry vehicle.

The 2-D model problem space is shown in Figure 1; the horizontal coordinate is z , the vertical coordinate is x , and the (third dimensional) y axis is perpendicular (and outward) to the plane of the figure. The initial conditions will consist of a sinusoidal TEM mode (truncated to one wavelength) in the parallel plate part of the horn. The plasma to the right of the dielectric slab has a gaussian profile in both the z and x directions. The physical

dimensions of the (square) 2-D space are 10 cm on a side and the TEM mode has a wavelength of 2.5 cm.

2-D Maxwell's Equations

For now, the magnetic permeability will be assumed to have only its free space value; in this case, the 2-D Maxwell's equations are (SI format):

<p>TM eqs.:</p> $\begin{aligned}\epsilon \partial_t E_x &= -\mu_0^{-1} \partial_z B_y - j_x \\ \partial_t B_y &= \partial_x E_z - \partial_z E_x \\ \epsilon \partial_t E_z &= \mu_0^{-1} \partial_x B_y - j_z\end{aligned}$	<p>TE eqs.:</p> $\begin{aligned}\partial_t B_x &= \partial_z E_y \\ \epsilon \partial_t E_y &= \mu_0^{-1} (\partial_z B_x - \partial_x B_z) - j_y \\ \partial_t B_z &= -\partial_x E_y\end{aligned}$
--	--

(1)

where the current j (and conductivity σ) are:

$$j(t) = \int_{-\infty}^t \sigma(t-\tau) E(\tau) d\tau; \quad \sigma(t) = \frac{1}{2\pi} \int_{-\infty}^{\infty} \bar{\sigma}(\omega) e^{-i\omega t} d\omega$$

(2)

Some initial conditions which can be used for the parallel plate wave guide of Figure 1 are:

<p>TM modes:</p> <p>TEM: $E_x = B_y, E_z = 0$</p> <p>TM₁: $k_1 = \frac{\sqrt{3}}{2} k, k = \frac{\omega}{c}$</p> <p>$E_x = \cos(k_1 z) \cos(\frac{1}{2} k x)$</p> <p>$B_y = \frac{2}{\sqrt{3}} \frac{E_x}{c}$</p> <p>$E_z = \frac{1}{\sqrt{3}} \sin(k_1 z) \sin(\frac{1}{2} k x)$</p>	<p>TE modes:</p> <p>TE₁: $k_1 = \frac{\sqrt{3}}{2} k, k = \frac{\omega}{c}$</p> <p>$B_x = \frac{\sqrt{3}}{2c} \sin(k_1 z) \sin(\frac{1}{2} k x)$</p> <p>$E_y = -\frac{2c}{\sqrt{3}} B_x$</p> <p>$B_z = \frac{1}{2c} \cos(k_1 z) \cos(\frac{1}{2} k x)$</p>
---	---

(3)

In the frequency domain, the complex 'permittivity' is defined in terms of the dielectric permittivity ϵ and conductivity σ as:

$$\bar{\epsilon}(\omega) \equiv \epsilon + \frac{i \bar{\sigma}(\omega)}{\omega} \quad (4)$$

where $\bar{\sigma}(\omega)$ is the Fourier transform of $\sigma(t)$ (and vice versa):

$$\sigma(t) = \frac{1}{2\pi} \int_{-\infty}^{\infty} \bar{\sigma}(\omega) e^{-i\omega t} d\omega \quad (5)$$

but ϵ is not the Fourier transform of $\bar{\epsilon}(\omega)$ (i.e., ϵ is always positive while $\text{Re}(\bar{\epsilon}(\omega))$ need not be). For a plane wave of angular frequency ω propagating in a plasma, a useful expression for $\bar{\sigma}(\omega)$ is [4]:

$$\bar{\sigma}(\omega) = i \frac{\epsilon_0 \omega_p^2}{\omega} \quad (6)$$

In the time domain, assuming a single frequency, we use for ϵ whatever the corresponding value is for that frequency; for $\sigma(t)$ in (2), we will use a constant value equal to $|\bar{\sigma}(\omega)|$ at the frequency of interest, $\omega = \omega_0$:

$$\sigma(t) = \sigma_0 \delta(t), \quad \sigma_0 = \frac{\epsilon_0 \omega_p^2}{\omega_0} \quad (7)$$

Thus, in (1), $\mathbf{j} = \sigma_0 \mathbf{E}$. In our numerical example, we will choose

$$\omega_p = 2\pi \times 25 \text{ GHz (maximum)} \quad \omega_0 = 2\pi \times 12 \text{ GHz}$$

so that at maximum electron density, $\sigma_0 = 3 \text{ mho/m}$.

The FCTD Method

The FCTD Method consists of a semi-implicit time integration scheme and a Fourier transform technique ("spectral method") for determining spatial derivatives. Here, spatial grids are $N \times N$, where N is a power of 2; in the numerical example we will use $N=128$. Since $\mathbf{j} = \sigma_0 \mathbf{E}$, the first TM equation in (1) can be written as, for example:

$$\epsilon \partial_t E_x = -\mu_0^{-1} \partial_z B_y - \sigma_0 E_x \quad (8)$$

When numerically integrating this, we can treat the last term on the right-hand-side implicitly, *i.e.*,

$$\epsilon E_x^{n+1} = \epsilon E_x^n - \Delta t [\mu_0^{-1} (\partial_z B_y^n) + \sigma_0 E_x^{n+1}] \Rightarrow E_x^{n+1} = \frac{\epsilon E_x^n - \Delta t \mu_0^{-1} (\partial_z B_y^n)}{\epsilon + \Delta t \sigma_0} \quad (9)$$

This first-order time integration is absolutely stable with respect to the conductivity; in fact, any non-negative value of σ is allowed on the model grid.

Following this example, a second-order time integration method for the TM equations in (1) is:

Predictor	Corrector
$E_x^{n+1/2} = \frac{\epsilon_r E_x^n - \frac{\Delta t}{2} c^2 (\partial_z B_y^n)}{\epsilon_r + \frac{\Delta t}{2} \frac{\sigma_0}{\epsilon_0}}$ $B_y^{n+1/2} = B_y^n + \frac{\Delta t}{2} (\partial_x E_z^n - \partial_z E_x^n)$ $E_z^{n+1/2} = \frac{\epsilon_r E_z^n + \frac{\Delta t}{2} c^2 (\partial_x B_y^n)}{\epsilon_r + \frac{\Delta t}{2} \frac{\sigma_0}{\epsilon_0}}$	$E_x^{n+1} = \frac{\epsilon_r E_x^n - \Delta t c^2 (\partial_z B_y^{n+1/2})}{\epsilon_r + \Delta t \frac{\sigma_0}{\epsilon_0}}$ $B_y^{n+1} = B_y^n + \Delta t (\partial_x E_z^{n+1/2} - \partial_z E_x^{n+1/2})$ $E_z^{n+1} = \frac{\epsilon_r E_z^n + \Delta t c^2 (\partial_x B_y^{n+1/2})}{\epsilon_r + \Delta t \frac{\sigma_0}{\epsilon_0}}$

(10)

The 1/2 time step values of the fields are only used as intermediate values and are not saved from one time step to the next.

The spatial derivatives in (10) are evaluated by a Fourier transform method; first, we transform to \mathbf{k} -space, find the Fourier coefficients of the derivatives of the fields, and then transform back to \mathbf{x} -space:

$$\bar{E}(\mathbf{k}) = \frac{1}{N} \sum_{\mathbf{x}} E(\mathbf{x}) e^{-i\mathbf{k} \cdot \mathbf{x}} \quad \Rightarrow \quad \nabla E(\mathbf{x}) = \frac{1}{N} \sum_{\mathbf{k}} i\mathbf{k} \bar{E}(\mathbf{k}) e^{i\mathbf{k} \cdot \mathbf{x}} \quad (11)$$

In (11) (and (12) below) we form a dyadic which can be specialized to a dot or cross product; also, $\mathbf{x} = 2\pi(j,k)/N$ ($0 \leq j,k \leq N-1$), and $\mathbf{k} = (m,n)$, ($N/2 - 1 \leq m,n \leq N/2$); j, k, m , and n are integers.

The Fourier transform method is equivalent to an N^{th} order finite difference method, if we view a generalized difference method as a convolution:

$$\nabla E(\mathbf{x}) = \sum_{\mathbf{x}'} \mathbf{D}(\mathbf{x} - \mathbf{x}') E(\mathbf{x}') \quad \mathbf{D}(\mathbf{x} - \mathbf{x}') \equiv \frac{1}{N^2} \sum_{\mathbf{k}} -i\mathbf{k} \sin[\mathbf{k} \cdot (\mathbf{x} - \mathbf{x}')] \quad (12)$$

However, instead of taking $O(N^2)$ operations for x -derivatives per point on an $N \times N$ grid, as the corresponding (N^{th} order) finite difference operation would, the number of operations (per point) is proportional to $N \log N$. The ratio of accuracy to time spent differentiating is thus much higher than the corresponding finite difference method. (The generic accuracy of spectral methods is well known [5], and will not be explicitly considered here.)

An FDTD method [1,2,3], has only second order spatial differencing, which makes it faster, but less accurate than the FCTD method described here. Another difference is that

in the FCTD method, both \mathbf{E} and \mathbf{B} are defined at the same physical grid point, while in the FDTD method, \mathbf{E} and \mathbf{B} are not defined at the same physical grid point, but rather 'leapfrog' over one another and lie on interleaved grid points.

Thus, in the FCTD method, \mathbf{E} and \mathbf{B} are *collocated* at all grid points. Collocation, however, also has another meaning in FCTD. In numerical analysis, a *collocation* method is a member of the *methods of weighted residuals*, and is also referred to as a *pseudospectral* method [6]. A collocation method assumes a solution in terms of known expansion functions and requires that the solution be exact (with respect to the function expansion) at the grid points; here, this means that we determine our spatial derivatives exactly (in terms of trigonometric functions). Since we are solving *time*-dependent equations, we have a *Fourier-collocation time-domain*, or FCTD, method. (If the equations were linear, which they are not because of the spatial variation of the material constants ϵ , μ , and σ , we would have a *Fourier-Galerkin* time-domain method [6].)

There are two kinds of boundaries in the model space. First, there are *interior* boundaries, *i.e.*, boundaries between various media within the model space. Second, there is the *exterior* boundary of the model space itself. In the numerical example to be presented here, the interior boundaries are linear, and at either 0, 45, or 90 degrees to the horizontal axis. Material properties (such as σ) are allowed to change discontinuously across the interior 0 or 90 degree boundaries, while on the 45 degree boundaries, material properties are set to a value halfway between those on either side of the interface (although this is not an essential part of the method). The exterior boundary, because of the use of a Fourier transform in evaluating derivatives, is periodic; this poses few problems, however, as long as the bulk of the model electromagnetic energy is contained naturally within the exterior boundary (as occurs in the numerical example to be presented). A problem with an open exterior boundary will require an algorithm for absorbing energy, or expansion functions other than trigonometric (or both), and is not addressed here.

Numerical Results

As a preliminary test case, the 2-D geometry shown in Figure 1 was set up. There are three essentially separate regions: a parallel plate microwave "horn" on the left of the figure, a dielectric slab of a relative permittivity of four in the middle of the figure, and a "plasma" to the right of the dielectric slab. The size of the numerical grid corresponding to Figure 1 is 128x128; the physical size of the grid is 10 cm on a side. The dielectric slab begins on horizontal grid point 52 and ends on grid point 84; this corresponds to about 2-1/2 cm. The lower corners of the horn are at (32,48) and (48,32), while the upper corners are at (32,80) and (48,96). The material of the horn is assumed to be solid and have a conductivity of 10,000 mhos/m at the transmission frequency of 12 GHz (although any value can be chosen). The plasma has a conductivity of

$$\sigma(z,x) = \sigma_o \exp\left[-(z-z_o)^2/2s_z^2 - (x-x_o)^2/2s_x^2\right]$$

$$\sigma_o = 3 (\Omega m)^{-1}, \quad z_o = 8.44 \text{ cm}, \quad x_o = 5.00 \text{ cm}, \quad s_z = 7.81 \text{ cm}, \quad s_x = 1.56 \text{ cm} \quad (13)$$

and is confined to the right-hand-side of the dielectric slab.

The results are shown in Figures 2 through 7. The simulation time step size was $\Delta t = 10^{-14}$ sec, the total number of time steps was 48,000, and the cpu time/time step was 0.164 seconds/ Δt (on a Cray-2). The total energy at the beginning of the simulation has a relative value of unity, and decreases as time wears on. The electromagnetic energy density, which is displayed in the Figures, is defined as

$$T_{EM} = \frac{1}{2}(\epsilon E^2 + \mu H^2) \quad (14)$$

T_{EM} can also be integrated over a selected region in physical space. This is done for the three disjoint regions of the model space: to the left of the dielectric slab, within the

dielectric slab, and to the right of the dielectric slab; this *regional energy* is given on each of the Figures.

It should be noted that there is a *reflected wave* in Figures 3 and 4 which barely shows up since its energy, which is small relative to the transmitted wave's energy, falls mostly below the lowest contour value in those Figures. The various reflections show up much better in Figures 5-7, as the primary wave has been greatly attenuated in the plasma to the right of the dielectric slab, and the relative energy of these reflections increases.

Conclusion

The results, as shown in the Figures, appear to be an accurate representation of the propagation of an electromagnetic wave through dielectric and conducting media (a 1-D test case with a linear grid of 2048 points, in which a plane wave was normally incident on a wide dielectric slab of relative permittivity 4, reproduced analytic predictions for reflection and transmission amplitudes to one part in 10^4). Material constants may be arbitrarily specified on a computational grid, so that practically any physical situation can be simulated. The FCTD method is of intrinsically higher accuracy than the FDTD method, as the FCTD method has (essentially) N^{th} order spatial differencing, while the FDTD method has only 2^{nd} order spatial differencing. While a 2-D example was presented here, it is a straightforward procedure to use the FCTD method for either 1-D or 3-D problems. (We should also note, at this point, that *finite element techniques* utilizing unstructured grids offer an alternative which may prove to be more efficacious, in general, than either FDTD or spectral methods.)

Although a Fourier transform method was used to evaluate derivatives, other function expansions (which may be more suitable for modelling certain boundary conditions) can be utilized (*e.g.*, Chebyshev polynomials); the FCTD method is thus only one example of a spectral method [7]. In the future, we plan to investigate the use of alternative function

expansions, as well as to investigate techniques for approximating absorbing boundary conditions and techniques for modelling the propagation of signals with broad frequency content. Applications which can be addressed include the simulation of microwave reflectometers interacting with the plasma generated in the bowshock of a hypersonic reentry vehicle.

Acknowledgements

The numerical data presented here came from computer runs performed on the NASA Ames Cray-2. The efficient transfer and visualization of numerical data was accomplished using the National Center for Supercomputing Applications (NCSA) Telnet and Imagetool software, respectively.

References

- [1] K. S. Yee, "Numerical Solution of initial boundary value problems involving Maxwell's equations in isotropic media", *IEEE Trans. Antennas & Propagation*, **AP-14**, 302-307, 1966.
- [2] A. Taflov, "Application of the finite-difference time-domain method to sinusoidal steady-state electromagnetic-penetration problems", *IEEE Trans. Electromagn. Compat.*, **EMC-22**, 191-202, 1980.
- [3] C. L. Britt, "Solution of electromagnetic scattering problems using time domain techniques", *IEEE Trans. Antennas & Propagation*, **AP-37**, 1181-1192, 1989.
- [4] J. D. Jackson, *Classical Electrodynamics*, 2nd Ed., p 287, Wiley, New York, 1975.
- [5] D. Gottlieb and S. A. Orszag, *Numerical Analysis of Spectral Methods: Theory and Application*, pp 135-8, SIAM, Philadelphia, 1977.
- [6] C. A. J. Fletcher, *Computational Galerkin Methods*, p 27 & p 205, Springer-Verlag, New York, 1984.
- [7] E. A. Coutias, F. R. Hansen, T. Huld, G. Knorr, & J. P. Lynov, "Spectral Methods in Numerical Plasma Simulation", *Physica Scripta*, **40**, 270-279, 1989.

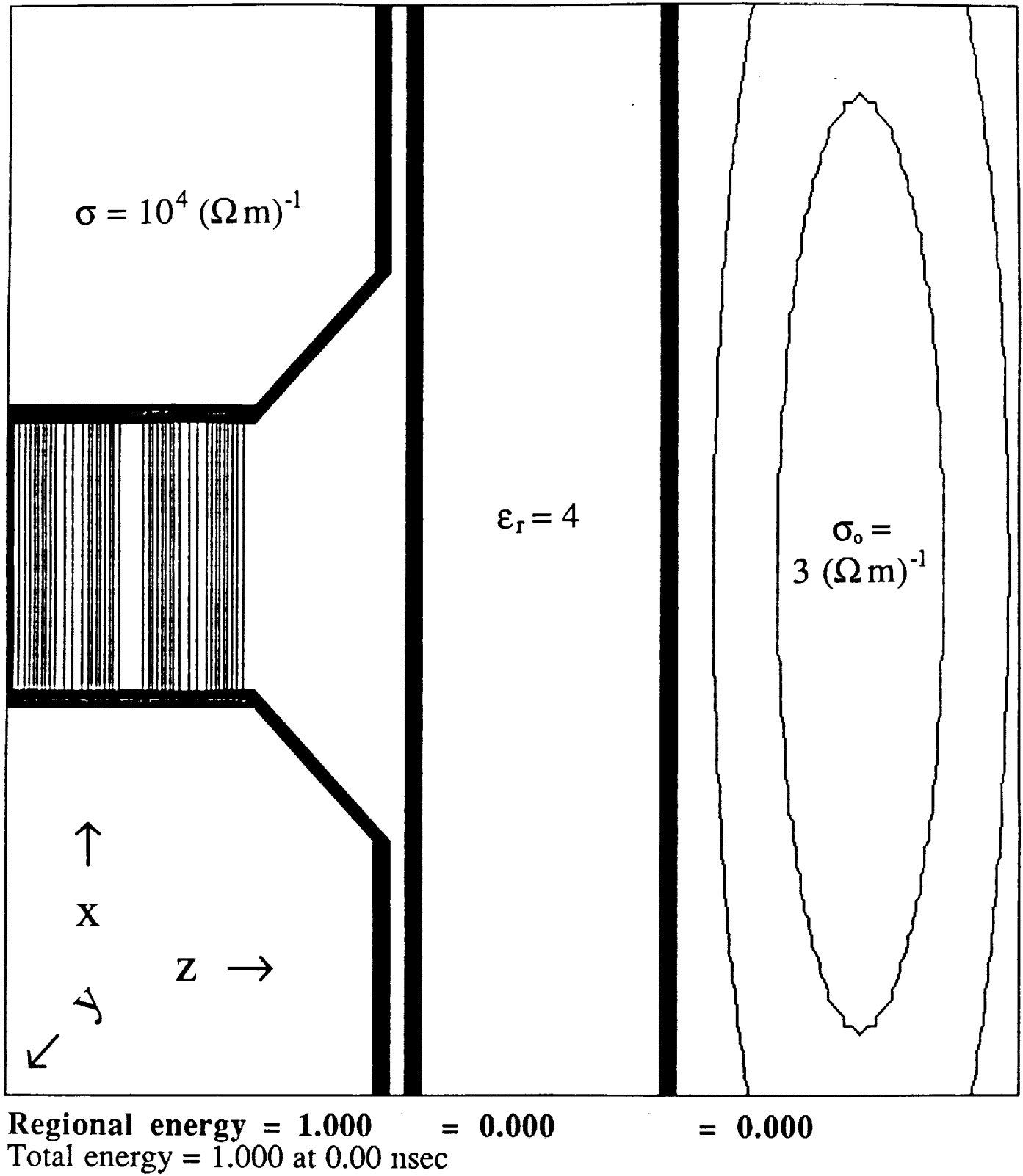
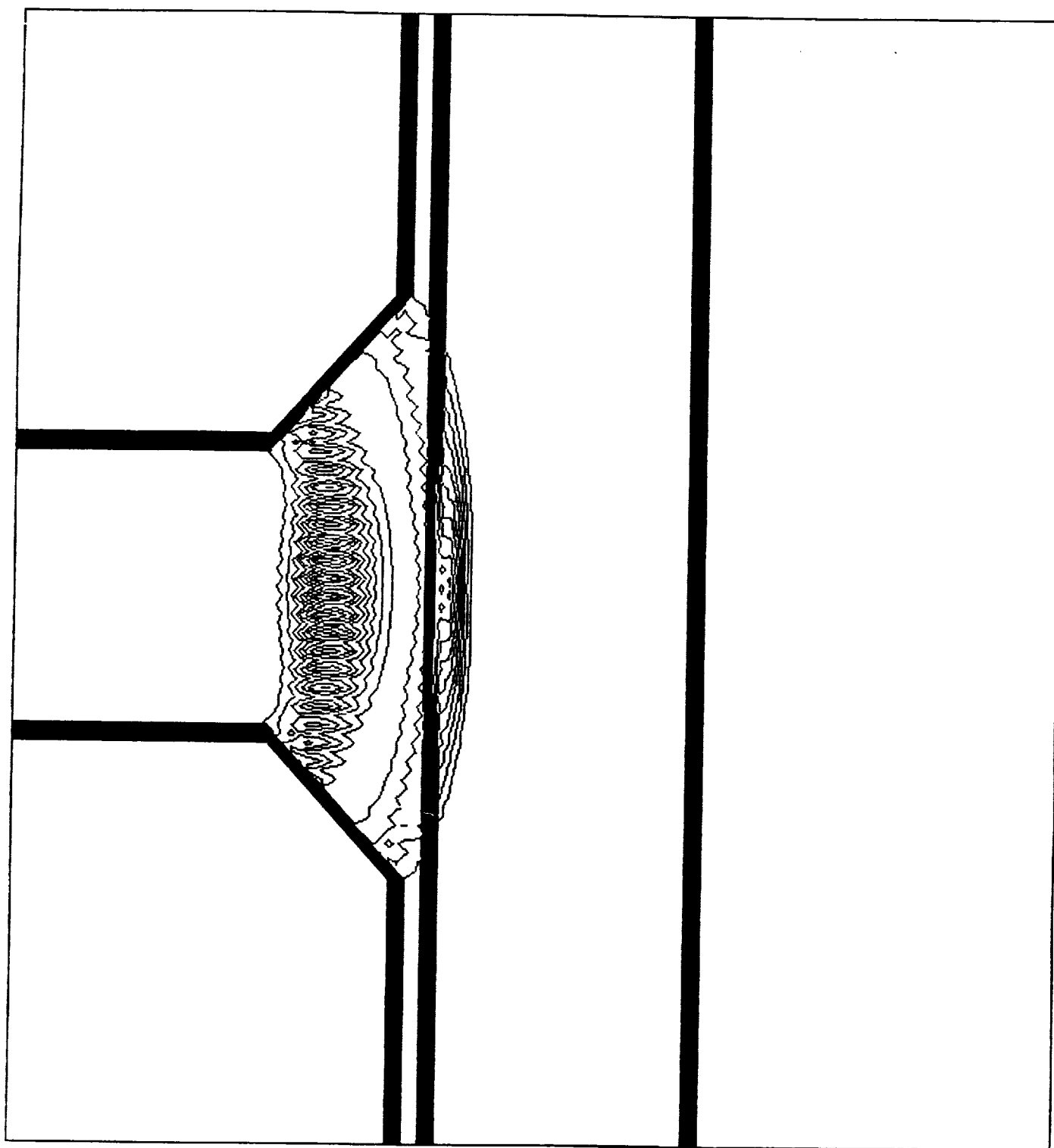
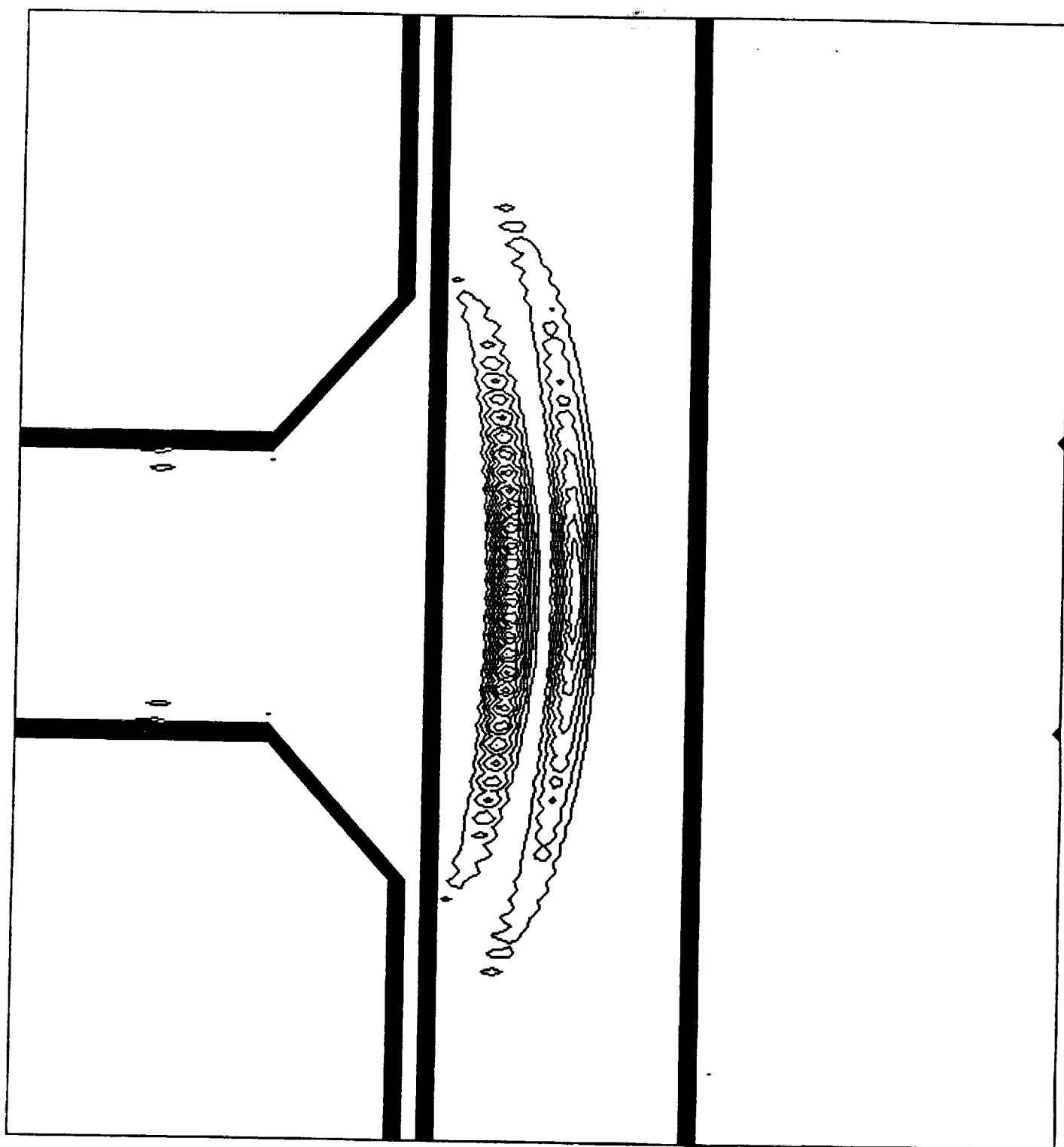


Figure 1. 2-D model space with initial energy distribution, along with permittivity and conductivity.



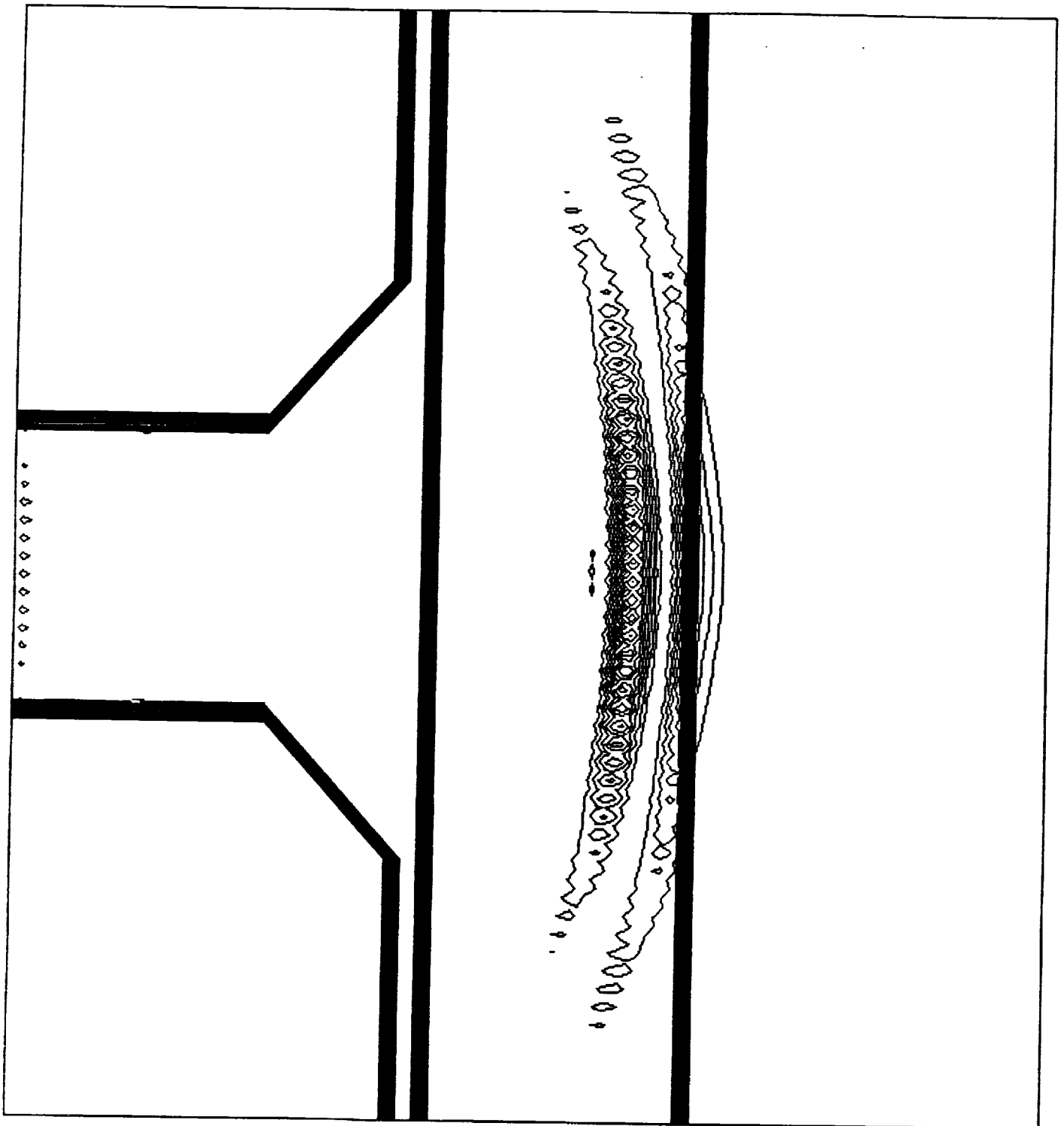
Regional energy = 0.696 = 0.301 = 0.000
Total energy = 0.997 at 0.08 nsec

Figure 2. Electromagnetic energy distribution at 0.08 nsec.



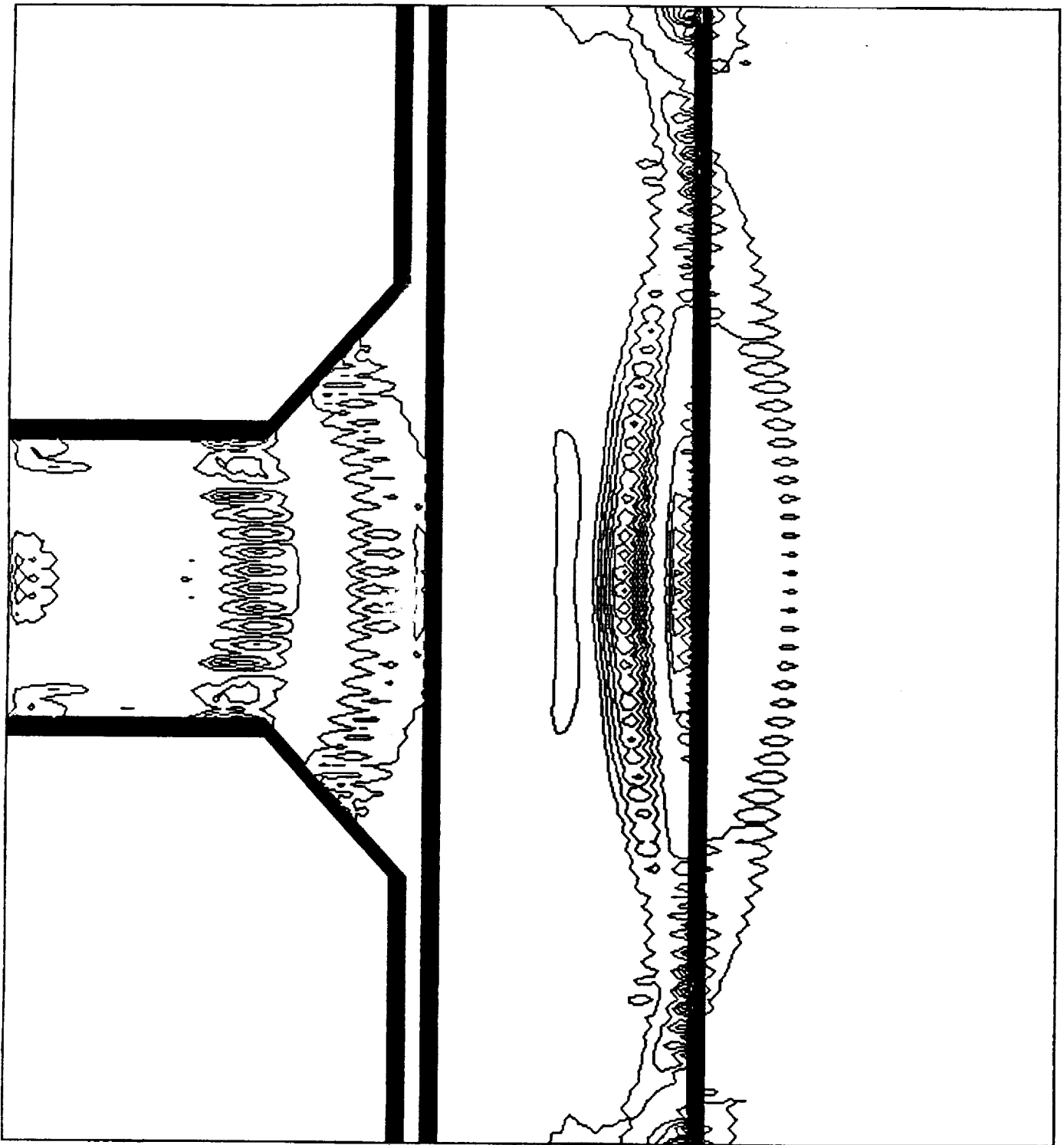
Regional energy = 0.128 = 0.858 = 0.001
Total energy = 0.987 at 0.16 nsec

Figure 3. Electromagnetic energy distribution at 0.16 nsec.



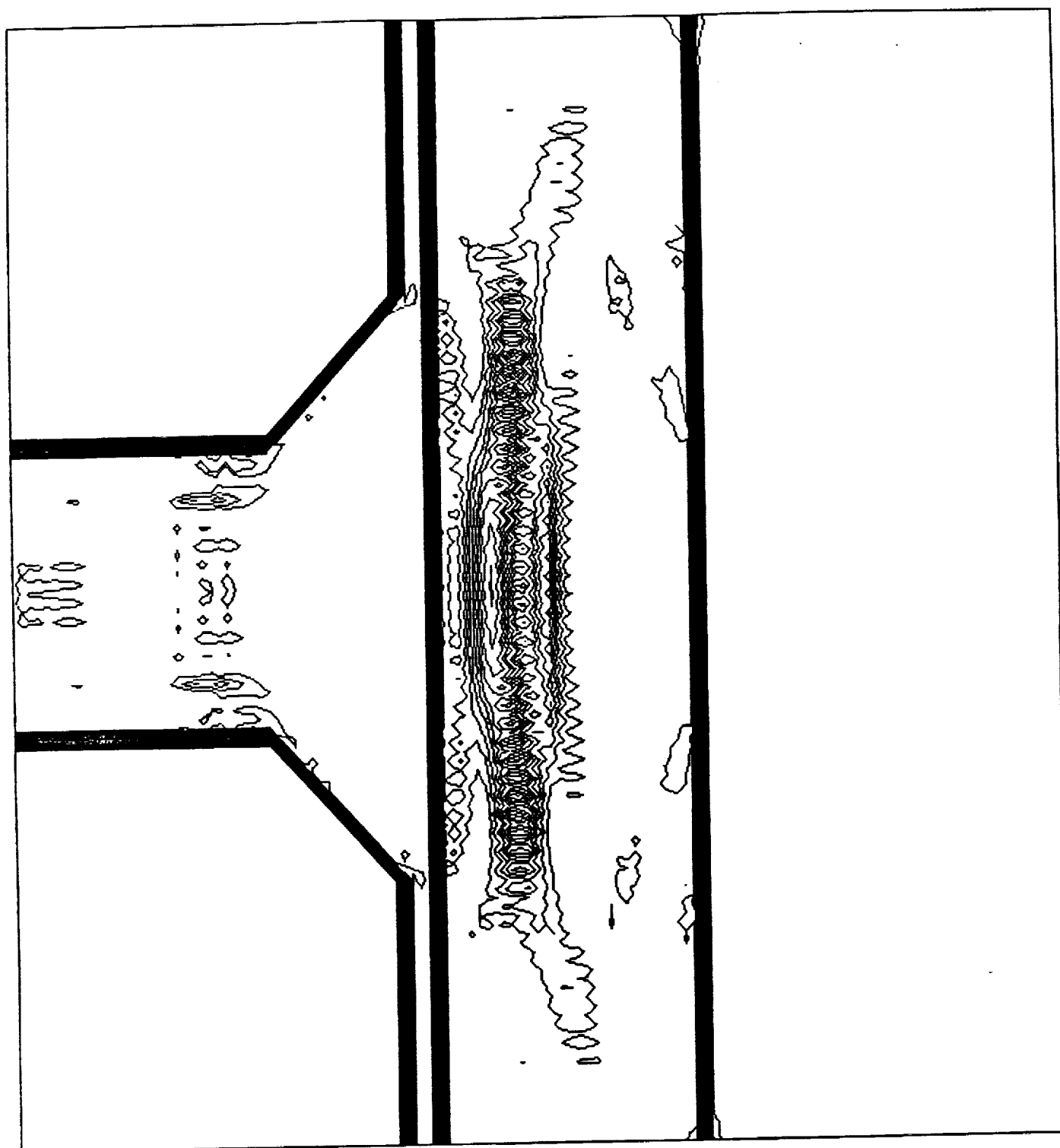
Regional energy = 0.094 = 0.785 = 0.074
 Total energy = 0.953 at 0.24 nsec

Figure 4. Electromagnetic energy distribution at 0.24 nsec.



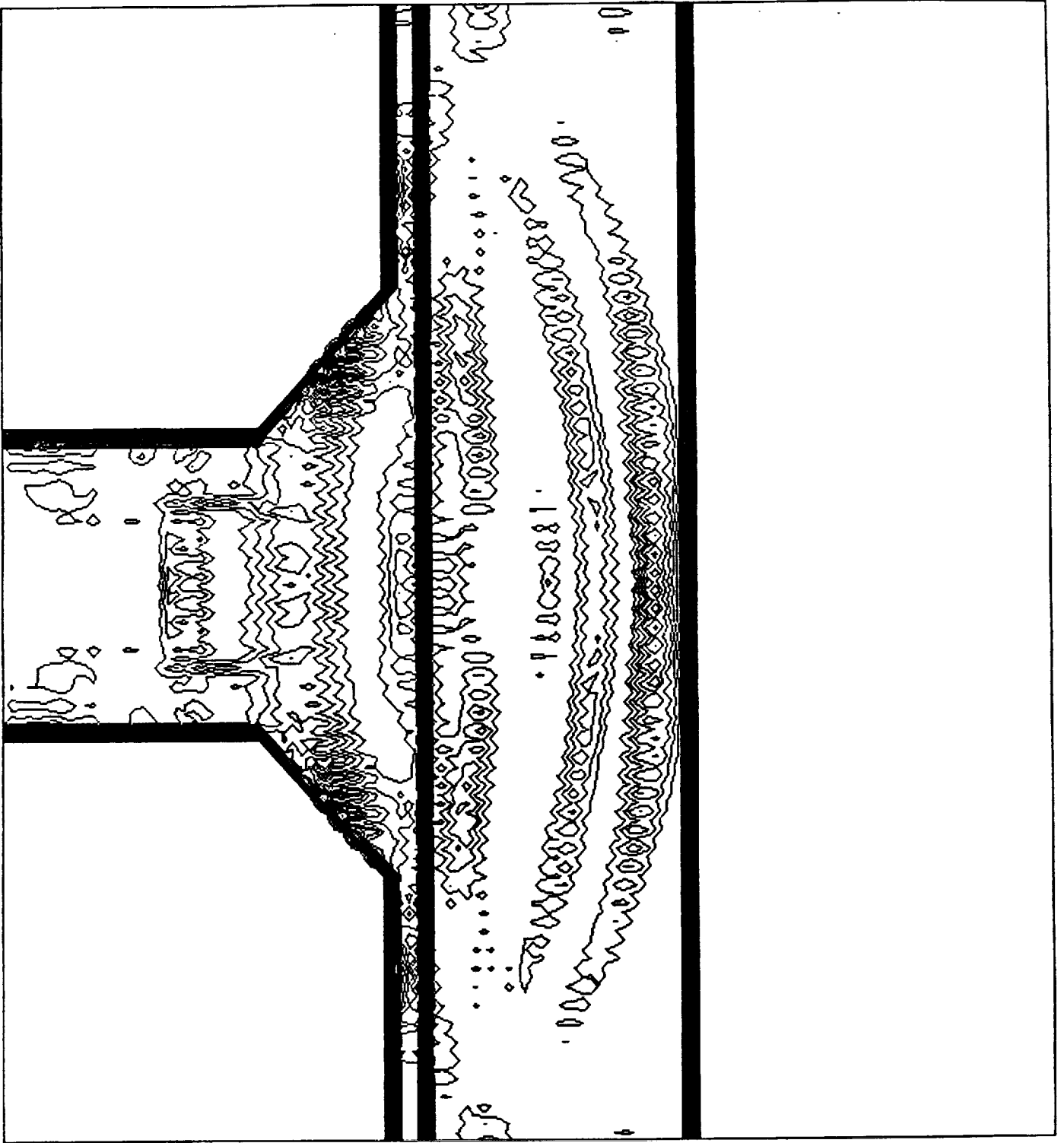
Regional energy = 0.082 = 0.171 = 0.053
 Total energy = 0.306 at 0.32 nsec

Figure 5. Electromagnetic energy distribution at 0.32 nsec.



Regional energy = 0.031 = 0.167 = 0.008
 Total energy = 0.206 at 0.40 nsec

Figure 6. Electromagnetic energy distribution at 0.40 nsec.



Regional energy = 0.086 = 0.093 = 0.004
 Total energy = 0.183 at 0.48 nsec

Figure 7. Electromagnetic energy distribution at 0.48 nsec.

REPORT DOCUMENTATION PAGEForm Approved
OMB No. 0704-0188

Public reporting burden for this collection of information is estimated to average 1 hour per response, including the time for reviewing instructions, searching existing data sources, gathering and maintaining the data needed, and completing and reviewing the collection of information. Send comments regarding this burden estimate or any other aspect of this collection of information, including suggestions for reducing this burden, to Washington Headquarters Services, Directorate for Information Operations and Reports, 1215 Jefferson Davis Highway, Suite 1204, Arlington, VA 22202-4302, and to the Office of Management and Budget, Paperwork Reduction Project (0704-0188), Washington, DC 20503.

1. AGENCY USE ONLY (Leave blank)		2. REPORT DATE October 1991	3. REPORT TYPE AND DATES COVERED Technical Memorandum	
4. TITLE AND SUBTITLE A Fourier Collocation Time Domain Method for Numerically Solving Maxwell's Equations			5. FUNDING NUMBERS WU 505-64-70-01	
6. AUTHOR(S) John V. Shebalin				
7. PERFORMING ORGANIZATION NAME(S) AND ADDRESS(ES) NASA Langley Research Center Hampton, VA 23665-5225			8. PERFORMING ORGANIZATION REPORT NUMBER	
9. SPONSORING/MONITORING AGENCY NAME(S) AND ADDRESS(ES) National Aeronautics and Space Administration Washington, DC 20546-0001			10. SPONSORING/MONITORING AGENCY REPORT NUMBER NASA TM-104162	
11. SUPPLEMENTARY NOTES				
12a. DISTRIBUTION/AVAILABILITY STATEMENT Unclassified - Unlimited Subject Category 64			12b. DISTRIBUTION CODE	
13. ABSTRACT (Maximum 200 words) A new method for solving Maxwell's equations in the time domain for arbitrary values of permittivity, conductivity, and permeability is presented. Spatial derivatives are found by a Fourier transform method and time integration is performed using a second-order, semi-implicit procedure. Electric and magnetic fields are collocated on the same grid points, rather than on interleaved points, as in the Finite Difference Time Domain (FDTD) method. Numerical results for the propagation of a two-dimensional Transverse Electromagnetic (TEM) mode out of a parallel plate wave guide and into a dielectric and conducting medium is presented.				
14. SUBJECT TERMS computational methods, electromagnetics, Fourier analysis			15. NUMBER OF PAGES 18	
			16. PRICE CODE A03	
17. SECURITY CLASSIFICATION OF REPORT Unclassified	18. SECURITY CLASSIFICATION OF THIS PAGE Unclassified	19. SECURITY CLASSIFICATION OF ABSTRACT	20. LIMITATION OF ABSTRACT	